

# FLUKA AND GEANT4 MONTE CARLO SIMULATIONS OF A DESKTOP, FLAT PANEL SOURCE ARRAY FOR 3D MEDICAL IMAGING\*

T. Primidis<sup>1†</sup>, C. P. Welsch<sup>1</sup>, University of Liverpool, Liverpool L69 3BX, UK  
V. Y. Soloviev, Adaptix Ltd, Oxford OX5 1PF, UK  
<sup>1</sup>also at The Cockcroft Institute, Warrington WA4 4AD, UK

## ABSTRACT

Digital tomosynthesis (DT) is a 3D imaging modality with a lower cost and lower dose than computed tomography. A DT system made of a flat panel array with 45 X-ray sources, but compact enough to fit on the desktop is near market realisation by the company Adaptix Ltd. This work presents a framework of FLUKA and Geant4 Monte Carlo (MC) simulations of the Adaptix system including the X-ray beam generation and the final image quality. The results show that MC methods offer an insight into the performance details of such an innovative device at different levels between the X-ray emitter array and the detector. As such, a large portion of the design and optimisation of such novel X-ray imaging systems can be done with a single toolkit. Finally, the modularity of the approach allows other tools to be imported at various steps within the framework and thus provide answers to questions that cannot be addressed by general-purpose MC codes.

## INTRODUCTION

Digital tomosynthesis (DT) is a modality similar to computed tomography (CT) where scans are taken within a limited angular range. Consequently, DT gives a form of 3D information for a much lower cost and dose than CT.

The X-ray tube has been the workhorse of 2D and 3D X-ray imaging for more than 100 years. This X-ray source is a large and heavy machine that needs cooling and stability mechanisms to control high machine temperatures and to reduce image artefacts from vibrations while it is rotated around the patient. The large size and weight of conventional X-ray tubes means that CT scanners only contain one source (or occasionally two). Even 2D and DT systems that use conventional tubes are also large and heavy, usually with a separate high voltage generator cabinet necessary.

However, Adaptix Ltd has demonstrated portable 3D DT imaging of human extremities, human jaws and small animals using a stationary flat panel source array and a stationary detector with systems that can fit on the desktop, as shown in Fig 1. The source array includes tens of cold-cathode field emitters etched on a Silicon wafer, each bombarding a transmissive X-ray target with electrons at energies between 60-70 keV. The sequential firing of emitters on the array produces X-ray beams that irradiate the

detector from different angles without rotation. Similar experimental systems exist that use a linear array of carbon nanotube field emitters [1]. However, it has been shown that a planar distribution of emitters improves depth resolution [2].



Figure 1: The Adaptix desktop tomosynthesis system. Courtesy of Adaptix Ltd.

Cold-cathode flat panel source arrays offer promising alternatives to X-ray tubes in medical applications. Also, numerical simulations can help improve the design and optimisation of this novel imaging technology [3].

In this paper, we describe a Monte Carlo (MC) simulation framework using the FLUKA [4] and Geant4 [5] codes to simulate the Adaptix imaging system, including X-ray beam production and image generation. We validate the models with experimental measurements and finally simulate a complete DT procedure, where 3D slices of a virtual fractured human extremity are reconstructed.

## METHODS

### *X-ray Beam Characterisation*

The exposed X-ray source and the corresponding MC model are shown in Figs. 2 and 3. All emitters were assumed to be identical so only one was simulated to characterise the entire array. The electron beam was defined as a 100  $\mu\text{m}$  wide Gaussian pencil beam at 60 keV, normal to the X-ray target and centred onto the collimator aperture. For simplicity, electromagnetic fields were not simulated. The position, direction and energy of photons that exited the printed circuit board (PCB) were scored in order to

\* Work funded by the Accelerators for Security, Healthcare and Environment Centre for Doctoral Training of the United Kingdom Research and Innovation, Science and Technology Facilities Council, reference ID ST/R002142/1

† thomas.primidis@liverpool.ac.uk

Content from this work may be used under the terms of the CC BY 3.0 licence (© 2021). Any distribution of this work must maintain attribution to the author(s), title of the work, publisher, and DOI

characterise the X-ray beam. This simulation was done with both FLUKA and Geant4 and the analysis that is described below was performed on their respective results.



Figure 2: The Adaptix flat panel source array exposed. Courtesy of Adaptix Ltd.

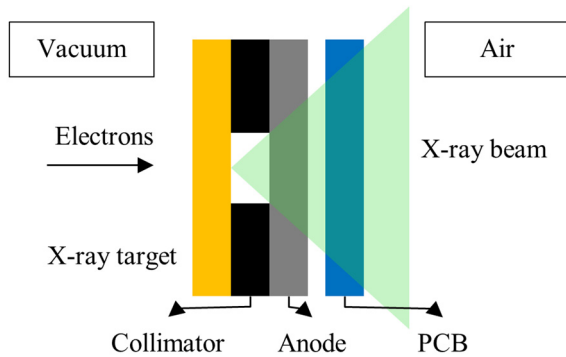


Figure 3: Model of a single X-ray source from the array. Illustration is not drawn to scale.

The X-ray beam was considered to be rotationally symmetric. Therefore, its shape was described by an analytical fit of the radial density of photons at the exit of the PCB. The fit included the beam core and the beam penumbra. Moreover, the energy for both, beam core and penumbra photons, was sampled from the analytical fit of the spectrum of the beam core. Also, to sample the photon direction, photons on the PCB were considered to originate from the centre of the X-ray target. The vector between these two points was the photon direction vector. Finally, the photon yield of the modelled source was the ratio of the number of photons exiting the PCB over the number of primary electrons transported.

### X-ray Beam Transport

Primary photon energy, position and direction was sampled using analytical fits. The number of photons emitted is the same for each source and calculated by multiplying the photon yield with the input current for the specific machine. Only the lateral position of each primary photon is shifted depending on the source position on the array.

### Model Validation

An RTI Black Piranha [6] dosimeter was used to measure the dose rate of the prototype flat panel source in the laboratory after attenuation of the beam in Aluminium. The dosimeter was placed 70 cm away from the X-ray source

and Aluminium sheets were placed between them. The experiment was replicated in FLUKA and Geant4 using the respective analytical source models.

### Digital Tomosynthesis

A phantom resembling a severely fractured extremity was placed in front of a flat panel detector. The detector covered a plane with 100  $\mu\text{m}$  pixels and standing 20 cm from the source array as shown in Fig. 4. Each pixel counted the photons incident in it, normalised by the angle of incidence. Images taken with the phantom in place were transformed into attenuation images by normalising them pixel-wise with respective images without the phantom in place using the same emitted photon flux. The pixel-wise negative natural logarithm of the normalised values then formed the attenuation images. For brevity and due to the agreement of the two analytical models which is shown later, DT was simulated only in Geant4.

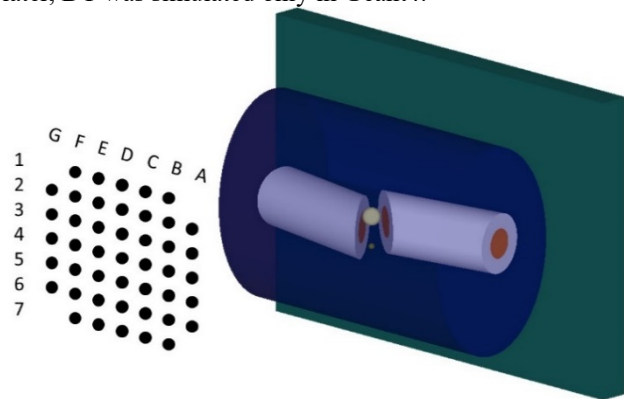


Figure 4: The modelled source array, phantom and flat panel detector. Emitter array is not drawn to scale.

To convert the multiple attenuation images into 3D DT slices, they were converted to 16-bit grayscale, uncompressed PNG images and were then input to a DT reconstruction algorithm [7]. The grayscale was linear with black end for pixel values less than or equal to 0 and with white end for pixel values greater than or equal to a threshold. This threshold was 1.2 times the 99 % limit of the pixel value distribution of all attenuation images. The 1.2 factor was used to avoid brightness saturation on some attenuation images, especially those from the outermost emitters such as A2 or A6 as shown in Fig 4.

## RESULTS

The radial photon density and the energy spectrum of the beam core for photons exiting the source are shown in Figs. 5 and 6. Both codes produce similar results. The radial density is fitted with polynomials within the beam core and with an exponentially decreasing function at the penumbra. A polynomial fit is used for the beam core energy spectrum. This is done separately for the results from each code.

The attenuation of the X-ray beam in the experiment and the simulations is shown in Fig. 7. The statistical error is smaller than the point size for all points. The two codes agree very well, but there is a factor of 4 discrepancy from

the experiment. The attenuation trend is similar between simulation and experiment. Therefore, the energy spectrum is estimated well, but the photon yield is not. Likely causes include the real electron beam being larger than the collimator aperture or only partially hitting the X-ray target due to misalignments. The simulated electron beam is perfectly centred onto the collimator aperture and thus all electrons arrive at the X-ray target.

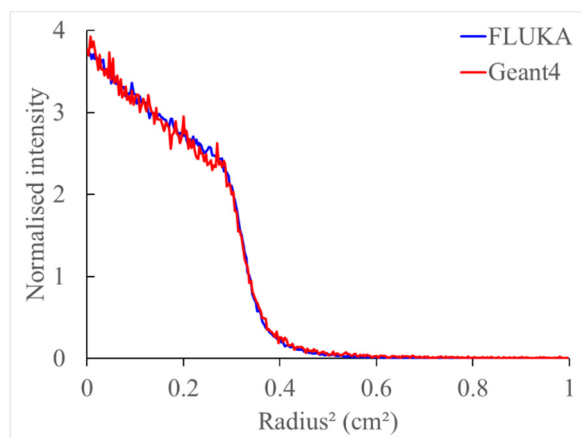


Figure 5: The radial photon density of the X-ray beam escaping from the source.

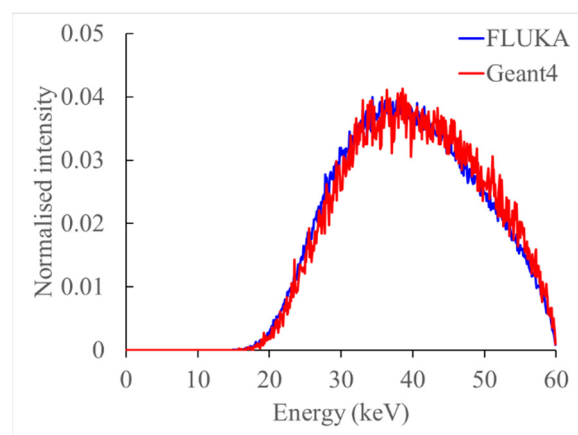


Figure 6: Energy spectrum of the beam core of photons escaping from the source.

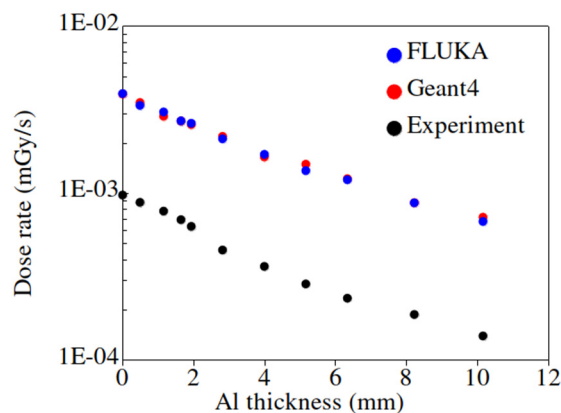


Figure 7: Attenuation of the X-ray beam in Aluminium.

DT slices are shown in Figs. 8 and 9. They are at different depths in the phantom and show the objects that correspond to their respective depth in focus. The spherical fragments are clearly delineated in focus within the cylindrical ones, identifying their depth within the phantom. A 2D X-ray image would show all of these structures overlapped, underlining the distinct advantages of DT.

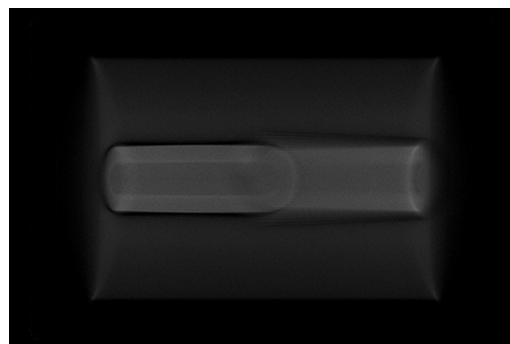


Figure 8: DT slice at the depth of the left bone.

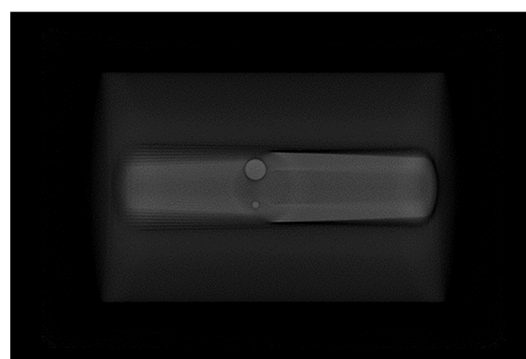


Figure 9: DT slice at the depth of the spherical fragments.

## CONCLUSION

A detailed MC simulation framework to assess and optimise the performance of compact X-ray emitter arrays was established and benchmarked against experimental data. X-ray generation, absorption in the patient, as well as image formation can all be modelled using a single tool, simplifying research and development. The framework can also be split into different modules, as described in the paper. This allows using other tools that can potentially provide better insight into specific optimisation targets such as electron field emission or the exact detector response. This provides an excellent avenue to complement general-purpose MC codes.

## ACKNOWLEDGEMENTS

This work was undertaken on Barkla, part of the High-Performance Computing Facilities at the University of Liverpool. Thomas Primidis is funded by the Accelerators for Security, Healthcare and Environment Centre for Doctoral Training of the United Kingdom Research and Innovation, Science and Technology Facilities Council, with reference number ST/R002142/1. The authors would like to thank Mr. James Cameron from Adaptix Ltd. for performing the dose rate measurements.

## REFERENCES

- [1] J. Shan *et al.*, “Stationary chest tomosynthesis using a carbon nanotube x-ray source array: a feasibility study”, *Phys. Med. Biol.*, vol. 60, pp. 81–100, 2014.  
doi:10.1088/0031-9155/60/1/81
- [2] S. Wells *et al.*, “Modelling the use of stationary, rectangular arrays of x-ray emitters for digital breast tomosynthesis”, in *Proc. SPIE, Medical Imaging 2020: Physics of Medical Imaging*, Houston, Texas, USA, Mar. 2020.  
doi:10.1117/12.2548438
- [3] E. Skordis, V. Vlachoudis, and C. Welsch, “A Monte Carlo approach to imaging and dose simulations in realistic phantoms using compact x-ray source,” in *Proc 8th Int. Particle Accelerator Conf.(IPAC'17)*, Copenhagen, Denmark, May 2017, pp.100-103.  
doi:10.18429/JACoW-IPAC2017-THPVA137
- [4] A. Ferrari, P. R. Sala, A. Fasso, and J. Ranft, “FLUKA: A Multi-particle transport code”, CERN-2005-10, USA, Rep. SLAC-R-773, Oct. 2005.
- [5] J. Allison *et al.*, “Recent developments in Geant4”, *Nucl. Instrum. Methods Phys. Res. Sect. A*, vol. 835, pp. 186–225, 2016. doi:10.1016/j.nima.2016.06.125
- [6] RTI Group, <https://rtigroup.com>
- [7] V. Y. Soloviev, K. L. Renforth, C. J. Dirckx, and S. G. Wells, “Meshless reconstruction technique for digital tomosynthesis,” *Phys. Med. Biol.*, vol. 65, p. 085010, 2020.  
doi:10.1088/1361-6560/ab7685